Extraction of Atmospheric Water On Mars
for the Mars Reference Mission

Sergio Adan-Plaza
Kirsten Carpenter
Laila Elias
Rob Grover
Mark Hilstad
Chris Hoffman
Matt Schneider

Professor Adam Bruckner

Department of Aeronautics and Astronautics
University of Washington, Box 352400
Seattle, WA 98195-2400

ABSTRACT

The University of Washington has designed an *in situ* resource utilization system to provide water to a life support system in the laboratory module of the NASA Reference Mission to Mars. This system, the Water Vapor Adsorption Reactor (WAVAR), extracts water vapor from the Martian atmosphere by adsorption in a bed of type 3A zeolite molecular sieve. The zeolite 3A adsorbs the water vapor until nearly saturated and is then heated within a sealed chamber by microwave radiation to drive off the water for collection. The water vapor flows to a condenser where it freezes and is later liquefied for use in the life support system. In the NASA Reference Mission, water, methane, and oxygen are produced for life support and propulsion via the Sabatier/Electrolysis process from seed hydrogen brought from Earth and Martian atmospheric carbon dioxide. In order for the WAVAR system to be compatible with the NASA Reference Mission, its mass must be less than that of the seed hydrogen and cryogenic tanks apportioned for life support in the Sabatier/Electrolysis process. The WAVAR system is designed for atmospheric conditions observed by the Viking missions, which measured an average global atmospheric water vapor concentration of $\sim 2 \times 10^{-6}$ kg/m^3. WAVAR performance is analyzed taking into consideration hourly and daily fluctuations in Martian ambient temperature and the corresponding effects on zeolite performance.

1. INTRODUCTION

Current plans to send humans to Mars rest on a mission architecture called the NASA Mars Reference Mission [1]. With concepts derived from Zubrin *et al's* Mars Direct mission architecture [2], the Reference Mission utilizes a strategy known as *in situ* resource utilization, or ISRU, which is defined as the use of indigenous resources at the site of an interplanetary mission for the production of life support consumables and/or rocket propellant [3]. In the Reference Mission, an ISRU process called the Sabatier reaction produces water from seed hydrogen brought from Earth and carbon dioxide from the Martian atmosphere [2]. This water is partially used for life support and the remainder is used for the production of rocket propellants.

Water needs on Mars in the Reference Mission require the production of 23,200 kg of water for life support from 2,600 kg of seed hydrogen imported from Earth [4]. This cache of water is intended to supply the water needs of three missions and is produced entirely by an original ISRU plant landed with the first cargo flight two years prior to the arrival of the first crew. While simple in principle, the importation of seed hydrogen to Mars is extremely challenging due to the need to cryogenically store liquid hydrogen for extended periods of time. A cryogenic hydrogen system having a boil-off rate of 0.5% per day requires leaving Earth with 7,008 kg of liquid hydrogen in order to reach Mars with 2,578 kg after a 200-day journey. This does not include boil-off that occurs on Mars. To make boil-off amounts tolerable, a presently unobtainable evaporation rate on the order of 0.1% per

day needs to be attained. With such a rate, delivering 2,600 kg of liquid hydrogen to Mars requires leaving Earth with 3,200 kg. NASA's current plan for liquid hydrogen storage rests on super-thermal cryogenic tank research that will maintain liquid hydrogen with no boil-off using active refrigeration [4], however, the mass and power required for this alternative may ultimately prove to be prohibitive.

Initially the Mars Reference Mission is completely dependent on seed hydrogen for water; however, as pointed out by its architects, a source of indigenous water is needed for the long term success of human Mars exploration. The purpose of this study is to examine how an ISRU concept called the Water Vapor Adsorption Reactor, or WAVAR, might be incorporated into the Reference Mission to meet this indigenous water need.

WAVAR is a process conceived and developed at the University of Washington's Department of Aeronautics and Astronautics under the guidance of A.P. Bruckner [5]. It obtains indigenous water by extraction from the Martian atmosphere. The atmosphere of Mars is the most highly characterized and global water source on the planet [6-8]. Both seasonal and daily cycles have been observed and the amount of water vapor has been found to vary strongly with latitude. The column abundance of water vapor was determined as a function of latitude for a period of nearly 1½ Mars years (~1000 days) by the Viking Orbiters [8]. The amount ranged from less than 1 *pr* μ*m* (precipitable micrometers) at high southern latitudes in midwinter to 100 *pr* μ*m* at high northern latitudes in midsummer. The seasonal variation of local humidity at the two Viking Lander sites was found to be in the range of $\sim 1.8 \times 10^{-7}$–2×10^{-6} kg/m^3 at VL-1 and $\sim 4 \times 10^{-10}$–3×10^{-6} kg/m^3 at VL-2 [9]. More recently Pathfinder measured a column abundance of ~10 *pr* μ*m* [10]. These numbers appear to indicate an extremely dry atmosphere compared to Earth's, but on the average, the atmosphere of Mars is holding as much water as it can on a daily basis, i.e., 100% relative humidity at night throughout the lowest several kilometers, at most seasons and latitudes [11]. The global average of atmospheric water is 0.03% by volume [6], corresponding to saturation at about 200 K, i.e., a concentration of $\sim 2 \times 10^{-6}$ kg/m^3. At the north polar regions during summer the concentration may exceed 10^{-5} kg/m^3. For this study the humidity data of Ryan *et al* at VL-1 and VL-2 were used [9]. In addition, hypothetical sites near the north pole and elsewhere showing enhanced humidities were also used, as described later.

Key to the WAVAR concept is the use of a molecular sieve adsorbent called zeolite, a strongly hydrophilic crystalline alumino-silicate commonly used in industrial dehumidifiers. As illustrated in Fig. 1, the WAVAR process is conceptually very simple. Martian atmosphere is drawn into the system through a dust filter by the fan. The filtered gas passes through the adsorbent bed, where the water vapor is removed from the flow. Once the bed has reached saturation, the water vapor is desorbed from the bed, condensed, and piped to storage. The design has only seven components: a filter, an adsorption bed, a fan, a desorption unit, a bed rotating mechanism, a condenser, and an active-control system.

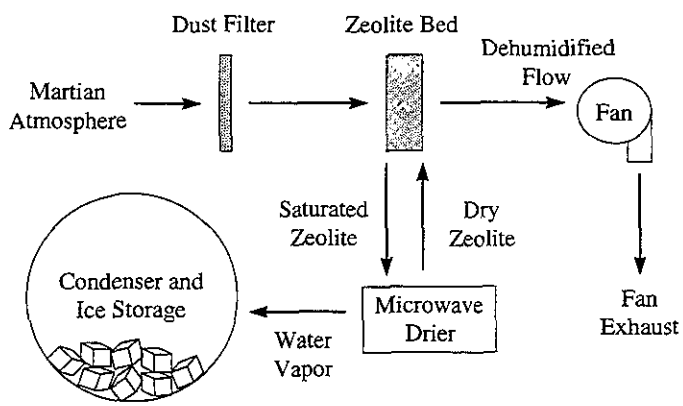

Fig. 1. The WAVAR process.

The WAVAR fan has to move a low humidity (~0.03% by volume), low temperature (~210 K), low pressure (~5 torr) gas, deal with frequent off-design operational periods, and work continuously and reliably for long periods of time (500-600 sols typical surface stay for low-energy Mars transfers). Because the flow will already be rigorously filtered to minimize fouling of the adsorption bed by Martian dust, abrasive wear on the fan can be kept to a minimum. The motor used for the WAVAR fan must operate over a range of loadings because of the variable nature of the ambient density [12].

Adsorption is a process which removes a species (the adsorbate) from a fluid as the fluid passes through a bed (the adsorbent). The adsorbent in WAVAR is zeolite 3A, a material which adsorbs water vapor but allows the other atmospheric gases (primarily carbon dioxide) to pass through. Section 2 provides further details about zeolites and the adsorption process. In the current WAVAR design, the pelletized adsorbent is packed into a bed placed in a radial flow configuration. This design is discussed in detail in Section 3.

Desorption of the bed is achieved by thermal swing desorption, which involves heating the bed until the thermal energy of the adsorbed molecules is greater than the adsorbent/adsorbate bond strength [13]. Thermal swing desorption is well suited for strongly adsorbed species such as water and can be accomplished either through resistive heating or with microwaves. The use of microwaves for the regeneration of zeolites has been demonstrated by Roussy, *et al* [14], and Whittington, *et al* [15]. The major advantage of using microwave energy over conventional conductive heating is that it provides rapid uniform heating for reduced desorption time and can be tailored to specifically heat water molecules.

The use of WAVAR on Mars has been the topic of past studies at the University of Washington, with most attention focused on its use in robotic sample return missions [5,16,17]. However, WAVAR is a process that is easily scaleable and has been included in one previous human Mars mission study [18]. In the present study, as a starting point for the incorporation of WAVAR into the Reference Mission, the water requirement needed to replace regenerative life support losses is set as a top-level design requirement. For a crew of eight, estimated losses amount to 6.5 kg per sol [19] over a typical surface stay duration of approximately 600 sols. Design of the physical configuration of a WAVAR system to meet this requirement is subject to several constraints. Among these constraints are system mass and footprint limitations, the adsorption capacity of zeolite 3A, the water needed to make up for life support regenerative losses, power limitations, minimization of moving parts, ease of integration into the NASA Reference Mission, and the overall simplicity and maintainability of the system and components.

The WAVAR configuration proposed by Williams, et al [5] was used as a starting point for the design. Redesign and optimization of the WAVAR is focused around four goals. First, the WAVAR must collect 3.3 kg of water per sol to make up for the water lost through life support regenerative processes. The WAVAR arrives at Mars with the laboratory habitat module, and begins operation immediately. The system then collects water for the next two years before astronaut arrival, as well as during the 500-600 sol human surface mission. This total of almost 4 Earth years of operation time reduces the daily water collection requirement by a factor of two as compared to a 500-600 sol operation during the human surface mission only. The mass flow rate of water vapor through the zeolite bed must be high enough to ensure an average net gain of 3.3 kg of water per sol during its operation time, enough to supply the astronauts with the water needed during the nominal surface mission. Second, the power drain of the system must be kept to a minimum. Power requirements are dominated by the need to transport large volumes of air through the filter and the zeolite bed (up to 1×10^9 m^3/kg-H_2O during the driest seasons), and the power required to desorb water from the zeolite. In order to minimize the pressure drops at the filter and bed and the corresponding fan power needs, flow velocities are kept low and the zeolite bed and dust filter are kept as thin as possible. Third, the WAVAR must be sized to fit on top of the current Reference Mission laboratory module to facilitate integration with the Mission and to simplify collection of the water for use in the life support system. Fourth, the mass of the WAVAR system must be less than that of the seed hydrogen it replaces in the current NASA Reference Mission. Table 1 summarizes the major quantitative design restrictions.

Table 1. Summary of quantitative system design constraints.

Characteristic	Restriction	Derived From
Net water gain	≥ 3.3 kg/sol	Mass of water needed daily over four years to make up for 600 sols of life support regenerative losses.
Average power drain	≤ 16 kW	5% of Reference Mission available power.
Footprint	≤ 7.5 m diameter	Habitat diameter is 7.5 m.
System mass	≤ 1200 kg	Reference Mission currently requires 1200 kg of seed H_2 to be launched from Earth for replacement of water lost in life support regenerative processes, assuming an H_2 boil-off rate of 0.5% per day over a 200 day Earth/Mars transit. WAVAR takes the place of this seed H_2.

2. ZEOLITE CHARACTERISTICS

The single most important component of the WAVAR unit is the zeolite bed, since it is what extracts the water from the Martian atmosphere. Zeolites are found naturally on Earth and can also be synthesized for specific functions [20]. Since zeolite is so important to WAVAR, its characterization is critical.

Zeolites are crystalline alumino-silicates with a three-dimensional interconnecting network structure of silica and alumina tetrahedra that contain many micropores (Fig. 2). Since zeolites have a crystalline structure, the pore openings are uniform and therefore permit adsorption discrimination based on the size and configuration of molecules in a system. This is a property unique to zeolites, and forms the basis for the name "molecular sieve." The chemical composition for the naturally occurring sodium zeolite is $Na_{12}[(AlO_2)_{12}(SiO_2)_{12}]\bullet 27\ H_2O$, where 27 is the number of water molecules adsorbed per unit cell of fully saturated zeolite [20]. The tetrahedra are formed by oxygen atoms surrounding a silicon or aluminum atom. Each oxygen has two negative charges and each silicon has four positive charges. The trivalency of aluminum causes the alumina tetrahedron to be negatively charged, requiring an additional cation to balance the system. Thus, cations such as potassium, calcium, lithium or sodium are the exchangeable ions of the zeolite [20].

Type A zeolites have two types of void spaces where adsorbed molecules are stored: the outer cages, called β-cages, and, the inner cages, called α-cages (Fig. 2) [5]. The size selectivity takes place at these spots [20]. In both the α- and β-cages the water molecules are held by van der Waals forces [21].

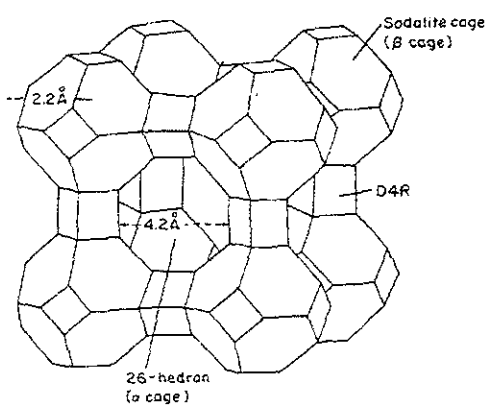

Fig. 2. The molecular structure of zeolite 4A [21]. The SiO_4/AlO_4 structure of the cage is the same for zeolite 3A and zeolite 4A. The substitution of larger potassium ions for the smaller sodium ions reduces the apertures of windows and cavities.

By controlling the ratios of cation exchange and the cation used, it is possible to synthesize zeolites containing different crystal structures. This property can regulate the pore diameter of the zeolite cavity and therefore selectively adsorb molecules of specific sizes.

For the WAVAR, a zeolite must be chosen that adsorbs water molecules but not the other species in the Martian atmosphere. The major constituent of the Martian atmosphere is CO_2 (95% by volume) and is the primary species to be excluded. As can be seen in Fig. 3, the only zeolite that can exclude CO_2 is the K type, which is a zeolite with most of the naturally occurring smaller sodium cations replaced by larger potassium cations. This reduces its average pore size to 3 Å which excludes the 3.3 Å size of CO_2 but accepts the 2.65 Å size of water [20]. Therefore, zeolite 3A was chosen to be the adsorbent for the WAVAR unit.

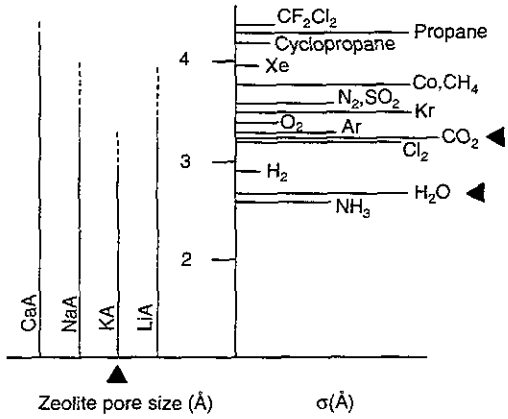

Fig. 3. Chart showing a correlation between effective pore size of various zeolites in equilibrium adsorption over temperatures of 77 K to 420 K (range indicated by ---), with the kinetic diameters of various molecules as determined from the L-J potential relation [20].

Zeolite Capacity

An important parameter of zeolite 3A is its capacity for water. Capacity is defined as the mass of water adsorbed per unit mass of dry zeolite. As can be seen in Fig. 4, the capacity of zeolite 3A varies strongly with both the ambient vapor pressure of water and the temperature. These data were obtained from a chart published by W.R. Grace Davison Molecular Sieves [22], having isotherms down to 253 K. The isotherms down to 170 K, represented by dashed lines, were obtained by logarithmically extrapolating the available data. These low temperature isotherms will need to be experimentally confirmed.

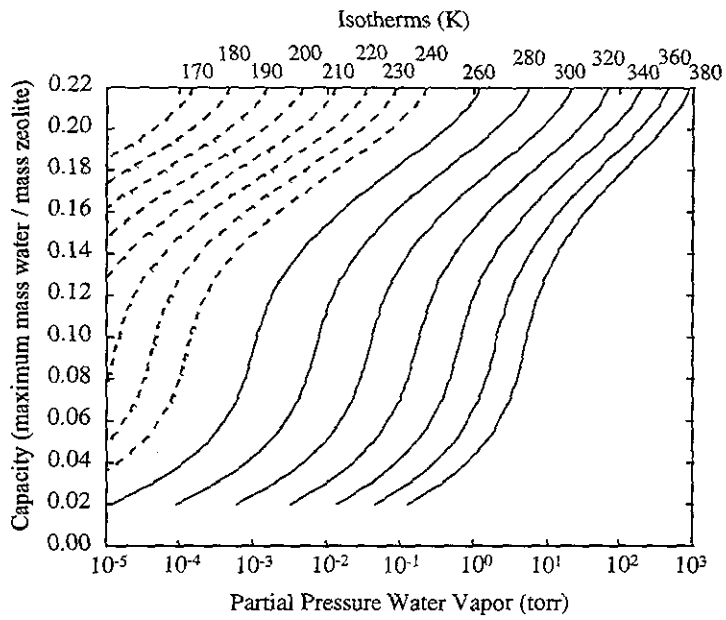

Fig. 4. Isotherms for capacity as a function of water partial pressure. The curves are from W.R. Grace Davison Molecular Sieves [22]. Dashed curves represent logarithmic extrapolations.

During a typical Martian day the temperature varies significantly and thus so does the water capacity of zeolite. Figure 5 shows the diurnal temperature variation on Sol 1 at the VL-1 site and the corresponding variation in the water adsorption capacity of zeolite 3A. As can be seen, the diurnal capacity fluctuation is large, which poses a problem for continuous running of the WAVAR unit. If it continued adsorbing through one of the low points in capacity (maximum ambient temperature), the zeolite would desorb down to what the maximum capacity was during that time. The condition in which the zeolite is loaded beyond its capacity due to a temperature drop is termed super capacity. During super capacity periods, the zeolite bed must be thermally isolated from the Martian ambient temperature so the zeolite does not heat up and the water prematurely desorb. This scheme is illustrated in Fig. 6, where the instantaneous water loading fraction is plotted over a period of four sols (Sols 4-8) at the VL-1 site. The two curves respectively show the capacity of the zeolite with its diurnal fluctuations, and the actual cumulative loading fraction with the bed insulated and inactive during the high temperature periods (horizontal curve sections). This problem increases the complexity of the WAVAR but it is unavoidable if the adsorption time is more than one sol, which for most places on Mars is the case. Figure 7 shows the holding capacity of zeolite 3A as a function of temperature for different partial pressures. The dependence of holding capacity on temperature and partial pressure is key to the design of the desorption process and will be examined in depth in future studies to determine optimum conditions for the process.

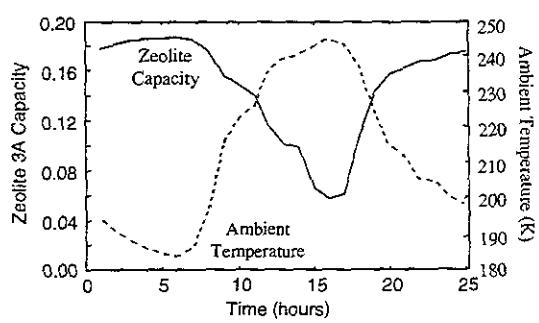

Fig. 5. Typical diurnal temperature variation (Sol 1 at VL-1) and corresponding zeolite equilibrium capacity.

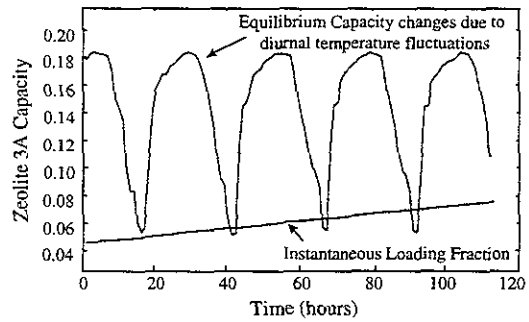

Fig. 6. Simulation results showing times when water capacity of zeolite drops below the current loading fraction, necessitating a method for thermal isolation of the zeolite bed.

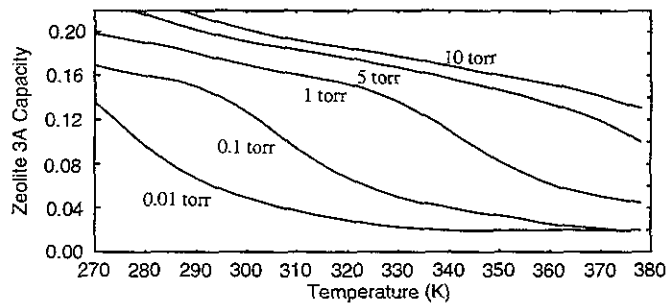

Fig. 7. Simulation showing zeolite capacity vs. temperature at different pressures.

3. SYSTEM DESIGN

3.1 WAVAR Geometry

The WAVAR is designed to minimize fan power requirements by providing a large area of zeolite through which the atmosphere can flow. A WAVAR design that operates efficiently and integrates cleanly with the NASA Reference Mission is shown in Fig. 8. The WAVAR uses a single fan to draw Martian air radially through a curved filter and bed of packed zeolite pellets, both shown in Fig. 9. The zeolite bed is a 180° arc, 10.8 m long, 0.93 m high, and 0.04 m thick, for a total bed flow area of 10.0 m^2 and mass of 240 kg. The annular structure that supports the four zeolite sections rests on rollers that are isolated from the dusty Martian environment. A stepping DC motor drives the rotation of the zeolite bed through a rack and pinion gear system, and a backup motor is available for emergency use.

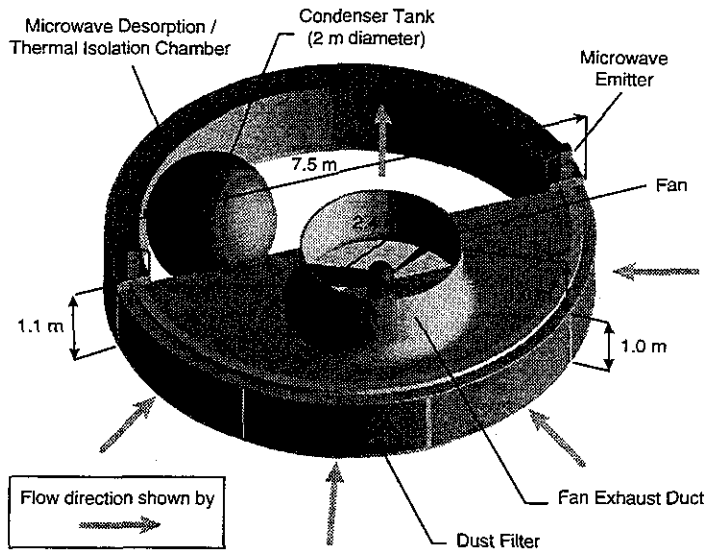

Fig. 8. WAVAR geometry and dimensions.

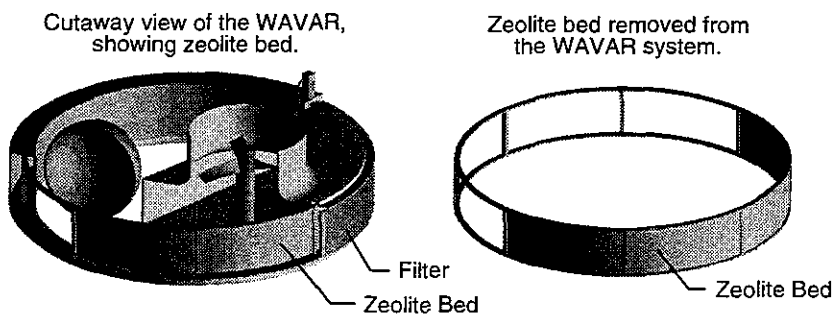

Fig. 9.. Zeolite bed location and shape.

The airtight desorption chamber shown in Fig. 8 is insulated from the temperature fluctuations of the ambient Martian environment, and is used for two purposes. The first use is for thermal isolation of the zeolite bed during the daily super-capacity hold cycle described above. When the bed reaches a super-capacity state due to an increase in ambient temperature, the fan stops and the bed rotates into the desorption chamber, located 180° about the WAVAR's central vertical axis. When the ambient temperature has dropped to beneath the super-capacity temperature, the bed rotates back 180° and the fan engages to continue the adsorption process.

The second use of the desorption chamber is for removal of adsorbed water from the zeolite bed. When a water loading fraction of 0.15 is reached, the zeolite bed rotates into the desorption chamber. During the desorption cycle, microwave emitters are used to heat and desorb the water from the zeolite bed. Initially the released water vapor freezes onto the walls of the desorption chamber, but further heating of the bed warms the walls of the chamber radiatively and sublimates this frost.

A variable-aperture valve links the desorption chamber with the 2 m diameter spherical condenser tank shown in Fig 8. A metal grid covering the valve opening prevents microwave radiation from entering the condenser. After the heating process begins, the valve opens to allow released water vapor to exit the chamber. The condenser is made of aluminum and remains exposed to the low temperature of the ambient Martian atmosphere. When the desorbed water vapor pressure reaches the saturation value, vapor begins to freeze on the cold condenser walls. This freezing maintains a pressure drop from the desorption chamber to the condenser, driving the vapor into the condenser. The rate of vapor transfer from the desorption chamber to the condenser is regulated by the variable-aperture valve to match the freezing rate so as to maintain this pressure difference between the de-

sorption chamber and the condenser. When as much water as possible has been desorbed from the zeolite, the valve between the desorption chamber and condenser closes. The zeolite bed rotates back into the airflow to be cooled and then to continue the adsorption process.

Adsorption, with intermittent hold and desorption cycles, continues for six months. Every six months or when necessary, the condenser is heated resistively to increase the vapor pressure and produce liquid water. A valve at the bottom of the condenser then opens that leads to a heated, pressurized liquid water storage tank within the laboratory module. The condensation and liquid water storage process is diagrammed in Fig 10. Prior to astronaut arrival, the liquid collection cycles are performed remotely. Liquification of the contents of the condenser results in a loss of 4.2 m^3 of habitat atmosphere as the atmosphere bubbles up through the valve into the condenser. This loss of atmosphere is not considered to be a problem because liquification need be performed only once every six months, and habitat atmosphere can be replenished relatively easily.

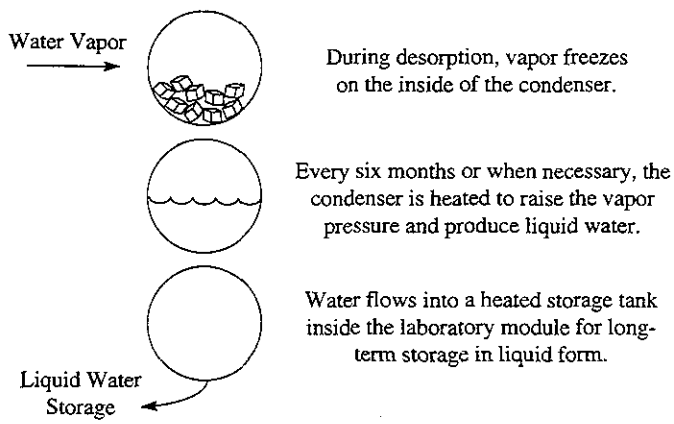

Fig. 10. Condensation and liquid water storage process.

The WAVAR is designed to fit on top of the Reference Mission laboratory module with minor changes to the current configuration. After integration with the existing structural supports on top of the module, the WAVAR increases the height of the module by about 0.5 m at the edges and 1.5 m at the exhaust duct, as shown in Fig. 11.

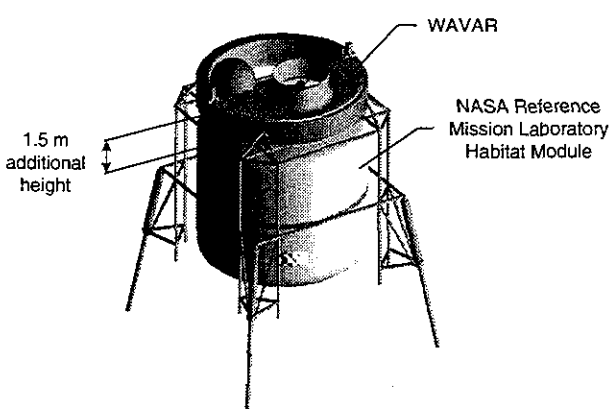

Fig. 11. WAVAR integration with the laboratory module of the NASA Reference Mission.

3.2 Desorption Process

To remove the adsorbed water from the zeolite bed, enough energy must be provided to break the bonds holding the water molecules in the bed. Thermal swing desorption is used due to its ease of implementation. The two types of heating processes considered were microwave and resistive wire heating. Heating by resistive wire is power and mass intensive due to the low thermal conductivity of zeolite. Microwave power was chosen for its controllability, specificity with water, and the relatively low mass necessary for its implementation. When heating the zeolite, there are two main considerations. The correct amount of power must be provided and the zeolite cannot be raised above the damage threshold temperature, ~600 K [23].

During desorption, the zeolite bed rotates into the insulated desorption chamber, where it is heated to 400 K. The desorption chamber is a microwave cavity resonator, and is sealed against the ambient environment for containment of desorbed water vapor. Heating reduces the water loading fraction in the bed to 1.5% (Fig. 7) [24]. Attempting to desorb to a lower percentage would take more power than is justified. The microwaves also heat the walls of the desorption chamber to prevent the liberated water vapor from condensing on the walls. The aluminum honeycomb walls absorb less than 1% of the total microwave power, and this power is input within a skin depth thickness of the walls. The desorbed water vapor enters a condenser and is later stored in the habitat for the astronauts' use, as discussed above.

3.2.1 Power Requirements

To desorb the water, the zeolite bed is heated to an average temperature of 400 K. This temperature provides enough energy to break the adsorption bonds, while preventing serious degradation due to thermal cycling over a four-years operational lifespan. The heating process begins with a bed at thermal equilibrium with Mars ambient conditions, i.e., an average temperature of 210 K. Initially, the microwave must provide enough energy to raise the temperature of the water and break the adsorption bonds. The zeolite bed is also heated to 400 K during the process. The heat of desorption of water is assumed to be equal to the heat of adsorption, found experimentally to be 4.19 MJ/kg [24]. The specific heat of water vapor was extrapolated to low temperatures from low-pressure data [25]. Table 2 lists the parameters used to compute the desorption power. The power required for desorption of the water over a four-hour period is:

$$Energy = C_{p\,zeolite} \cdot m_{zeolite} \cdot \Delta T + m_{H20}\left(\Delta H + C_{p\,H20} \cdot \Delta T\right) = 317\ MJ$$

$$Power = \frac{Energy}{t_d} = 22\ kW$$

Table 2. Constants assumed for desorption performance calculations.

$C_{p\,zeolite}$	Specific heat of zeolite [20]	3.375 kJ/kg·K
$C_{p\,H20}$	Specific heat of water vapor	1.854 kJ/kg·K
ΔH	Water heat of desorption	4.19 MJ/kg
$m_{zeolite}$	Total zeolite mass	240 kg
m_{H20}	Total water mass	36 kg
$T_{desorption}$	Maximum temperature	400 K
$T_{ambient}$	Mars ambient temperature (avg.)	210 K
ΔT	$T_{desorption}$ - $T_{ambient}$	190 K
t_d	Desorption cycle time	4 hours

3.2.2 Microwave Heating of Zeolite

Microwaves are electromagnetic (EM) waves operating in the gigahertz (GHz) frequency range. Water has a maximum absorption at 2.45 GHz; therefore the microwave operates at this frequency, similar to microwave ovens found in most kitchens. When heating a dielectric material with microwaves, certain considerations are needed in the design of an efficient, low mass system. The microwaves must penetrate throughout the volume of the bed, the power absorbed by the zeolite and water should be a substantial amount of the input power, the radiation impinging on the surface should be uniform, and the system that delivers the radiation should be as loss-free as possible.

As with most materials, zeolite is a dielectric [20]. EM wave propagation through dielectric materials can be represented by an oscillating electric field function that has an exponentially decaying amplitude. The complex dielectric constant, $\varepsilon' - j\varepsilon''$ [26] has a real and an imaginary permittivity term. The real term is the oscillation and the imaginary term is the exponential decay. The exponential decay represents the loss of power due to absorption by the dielectric. The distance from the input face to the location where the electric field is reduced by a factor of e^{-1} is called the skin depth, δ. The fraction of input power absorbed depends on this parameter as well as the bed depth, L.

$$\frac{P_{abs}}{P_{in}} = 1 - e^{-\frac{L}{\delta}}$$

Due to the lack of data on the electrical properties of zeolite 3A, data available for zeolite A was used. In general, ε' and ε'' depend on the frequency, temperature, and water content in the zeolite [20]. The value of ε'' represents the absorption by zeolite and water. At the frequency of interest, the permittivities become dependent on only one variable and become linear. At a water loading fraction of 0.15 and a temperature of 210 K, 40% of the input power is absorbed by a zeolite bed of 4 cm thickness.

Because only 40% of the input energy is absorbed during each pass, the desorption chamber is used as a microwave cavity to create a resonating field so that all the input power is absorbed by the water and the zeolite. Due to the shape and dimensions of the cavity, a specific field distribution resonates at 2.45 GHz. This is quantified by the mode numbers in the radial, azimuthal and axial directions. A waveguide transmits microwave power from the emitter and guides it to the desorption chamber, and an isolator prevents radiation from transmitting back and causing damage to the emitter.

3.2.3 Microwave Geometry

A magnetron microwave generator was chosen for its compactness and high power conversion efficiency of around 80%. Two magnetrons are used for redundancy and longevity. Each emitter is capable of supplying enough power for desorption by itself, but both are used simultaneously at half power to reduce wear from thermal cycling and overheating. The magnetrons are thermally isolated from the environment by an aluminum honeycomb shroud. The mass of a 25 kW magnetron is 20 kg, for a total of 40 kg for both. The magnetrons require a total input power from the main power grid of 27.8 kW, with each operating at half capability. In order to irradiate the large surface area of the zeolite in the desorption chamber, a combination of a waveguide and a cavity resonator (the desorption chamber) is used.

The magnetron emits a cylindrical wave from a cylindrical antenna [26]. A rectangular aluminum waveguide directs the transmission wave through an isolator. The waveguide is sized so that the microwave frequency is twice the geometric cutoff frequency of the waveguide. The waveguide cannot propagate EM waves at a frequency below the cutoff frequency. This frequency is obtained by solving Maxwell's equations for closed volumes, and depends only on geometry. The isolator prevents reflected waves from the resonating (desorption) chamber from transmitting back to the emitter by redirecting them into the terminator. The power is then transmitted through a small inlet waveguide and into the resonator. This input excites the resonant frequency of the desorption chamber, which is roughly 2.45 GHz, and the zeolite bed is bathed in radiation for four hours. Due to the geometry of the chamber, the actual resonant frequency will vary slightly from the optimum value. The reso-

nant frequency also excites high mode numbers of 10-20 in the radial and axial directions.

3.3 Materials and Mass

The WAVAR system must have a mass less than that of the seed hydrogen and associated storage systems required to make up for water losses in the life support system of the NASA Reference Mission. Regenerative losses amount to 6.5 kg H_2O per sol [19] while the crew is on the surface of Mars. For a surface stay of 600 sols this amounts to a total of 3900 kg of replacement water, requiring the use of 433 kg of seed H_2 for water production. Assuming a boil-off rate of 0.5% per day in transit to Mars, a launch from Earth of 1200 kg of seed hydrogen would be needed. Taking into account additional boil-off after arrival on Mars, this figure would increase. The aim of this design was to limit the mass of the WAVAR to 1200 kg.

The WAVAR system (Fig. 8) has a support structure made of two tubular aluminum circles spaced apart by tubular aluminum cross members, with the bottom plate of the adsorption chamber made of graphite-epoxy facesheets with Nomex honeycomb core [27]. The top of the adsorption chamber converges to the fan duct, which is made of the same honeycomb sandwich structure. The fan itself is made of graphite epoxy. The air filter, a Filtrete Type G from 3M [28], surrounds half the periphery of the WAVAR. All exterior components are flush mounted to the structural supports to prevent inflow of dust to the system. Inside the filter is the curved zeolite bed. An aluminum rack reinforced with steel facing under the zeolite bed is used with a stepping motor for rotation of the bed into the microwave desorption chamber.

The desorption chamber is completely encased and insulated from the rest of the WAVAR system and the Martian atmosphere. The walls of the chamber are composed of 0.25 mm thick sheet aluminum (inside), 3 cm thick Aerogel-Based Superinsulation and graphite-epoxy facesheets with a Nomex honeycomb core. These layers are illustrated in Figure 12. Aerogel-Based Superinsulation has a very low thermal conductivity, less than 0.1 mW/m-K, and a density of 12 to 35 kg/m^3 [29]. A density of 20 kg/m^3 was assumed for the mass estimate. Desorbed water vapor freezes in an aluminum condenser tank. The mass breakdown of the WAVAR system is summarized in Table 3.

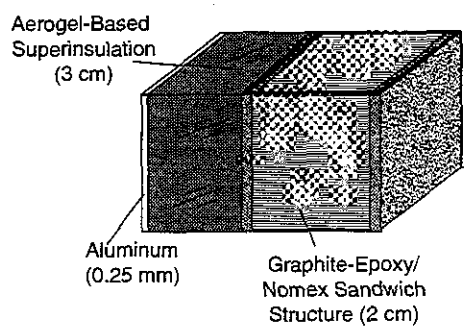

Fig. 12. Desorption chamber wall components.

Table 3. Summary of WAVAR system mass.

Component	Mass (kg)
Structural Supports	60
Adsorption Chamber Floor, Ceiling, and Duct	85
Dust Filter	10
Zeolite Bed	240
Bed Support Structure and Rack	120
Fan	30
Fan Motor (10 kW)	30
Desorption Chamber	150
Bed Rotation Motors (2)	10
Microwave Emitters (2)	40
Condenser Tank	100
Active Control System	10
TOTAL	**885**

4. PERFORMANCE

4.1 Fan Modeling

Achieving a high fan efficiency under WAVAR operational conditions is critical for the minimization of WAVAR power requirements. The design of the fan is driven by the need to efficiently transport large volumes of low density Martian atmosphere at the high velocities required by adsorption design constraints. A fan was designed using momentum-blade element theory, with modifications intended to take into account the rotation induced in the flow by fan rotation. The fan is optimized for operation at an axial flow velocity of 20.6 m/s, corresponding to a velocity at the zeolite bed of 9 m/s.

The 2.4 m diameter WAVAR fan consists of 3 rectangular blades of 0.3 m chord length, as shown in Fig. 13. The fan operates at 500 RPM, corresponding to an angular velocity of 52.4 rad/s. Blade angle of twist varies from 68.63° at the root to 23.47° at the tip, as given by:

$$\beta = -38\ln(0.3r + 0.015) + 16r - 33,$$

where r is the distance from the hub axis in meters and β is determined in degrees.

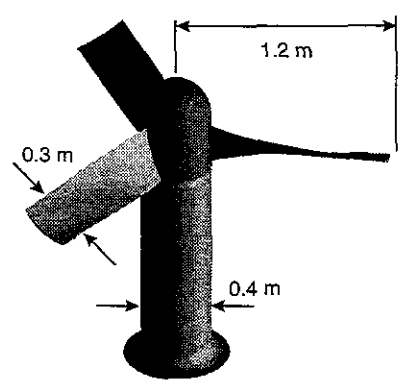

Fig. 13. WAVAR fan as modeled for simulations.

The basic equations of momentum-blade element theory are as follows, and are based on the geometry shown in Fig. 14 [30].

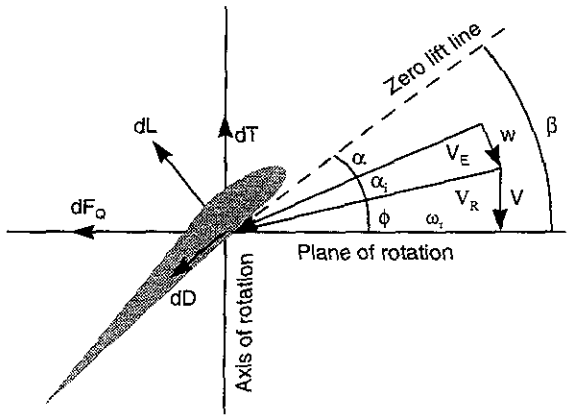

Fig. 14. Notation used for fan blade analysis [30].

$$\lambda = \frac{V}{\omega R} \qquad x = \frac{r}{R} \qquad V_T = \omega R$$

$$V_R = V_T\sqrt{x^2+\lambda^2} \qquad \sigma = \frac{Bc}{\pi R} \qquad \phi = \arctan\frac{\lambda}{x}$$

$$\alpha_i = \frac{1}{2}\left[-\left(\frac{\lambda}{x}+\frac{\sigma a V_R}{8x^2V_T}\right)+\sqrt{\left(\frac{\lambda}{x}+\frac{\sigma a V_R}{8x^2V_T}\right)^2+\frac{\sigma a V_R}{2x^2V_T}(\beta-\phi)}\right]$$

$$dL = \frac{1}{2}\rho V_R^2 c C_l dr \qquad dD = \frac{1}{2}\rho V_R^2 c C_d dr$$

$$dT = dL\cos(\phi+\alpha_i) - dD\sin(\phi+\alpha_i)$$

$$dQ = r\left[dL\sin(\phi+\alpha_i) + dD\cos(\phi+\alpha_i)\right]$$

$$P = \omega Q \qquad \eta = \frac{TV}{P}$$

where T is thrust, Q is torque, P is input power, and η is fan efficiency [30].

These equations are sufficient to solve for the fan efficiency if given the blade geometry, rotational speed, and axial flow rate [30]. To determine the axial flow velocity, the following formulation was used.

Given the angle of twist β and the chord length *c*, the volume swept out by a blade in one revolution is

$$\int_{R_1}^{R_2} dVol'$$

for the differential volume element

$$dVol' = 2\pi r c \sin\beta\, dr\,.$$

For *B* blades with ω angular velocity, this leads to an average axial flow velocity of

$$V' = \frac{\omega B\int_{R_1}^{R_2} dVol'}{\pi\left(R_2^2 - R_1^2\right)},$$

where R_1 is the hub radius and R_2 is the fan radius.

However, neither this velocity formulation nor momentum-blade element theory takes into account the decrease in axial velocity due to the tangential velocity imparted by the rotation of the fan. In order to approximate this loss, a factor of cos β is applied to the differential volume element *dVol*. With an angle of twist of 90° and slow rotation, this leads to an axial velocity of 0 m/s, as would be expected intuitively. At very small angles of twist, tangential velocity is minimized, also satisfying intuition. At high rotation rates, a factor taking into account α_i may provide a better approximation because of the effects of the induced angle of attack, but α_i in turn depends on the flow velocity. Including the rotational correction factor cos β, the equation for average axial velocity *V* becomes

$$V = \frac{\omega B \int_{R_1}^{R_2} dVol}{\pi\left(R_2^2 - R_1^2\right)}$$

where

$$dVol = 2\pi r c \sin\beta \cos\beta \; dr \, .$$

The choice of a specific airfoil for the fan blades was constrained by the need to operate in the low Reynolds number environment on the Martian surface. For V_R as defined above and blade chord length *c*, the Reynolds number was taken to be:

$$\mathrm{Re}_f = \frac{\rho V_R c}{\mu} \, .$$

The Reynolds number across the fan blades varies linearly with respect to radial position, from 1.09×10^4 at the root to 3.12×10^4 at the tip. At Reynolds numbers on the order of 2×10^4, a sharp leading edge rather than a sharp trailing edge produces more lift [31]. At Reynolds numbers in this regime, a circular arc airfoil with 5% camber provides a high lift to drag ratio [31], so this airfoil was chosen for use in the WAVAR fan. Fourth order curve fits to empirical lift and lift to drag ratio data with respect to angle of attack are shown in Fig. 15.

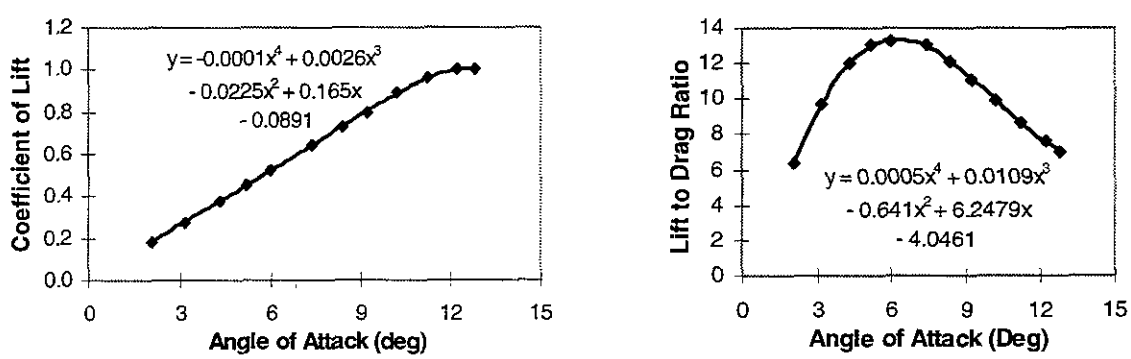

Fig. 15. Curves fit to empirical lift and lift to drag ratio data on 5% camber circular arc airfoil at Re = 2.07×10^4 [31].

An analysis of the WAVAR fan using the velocity equation derived above, momentum-blade element theory, and curve fit data for C_L and L/D leads to a fan efficiency of 76%. The major physical and performance characteristics of the WAVAR fan are summarized in Table 4.

Table 4. Fan calculation constants and results.

Symbol	Value	Explanation
ρ	0.017 kg/m^3	Mars ambient density
μ	1.08×10^{-5} N·s/m^2 [41,42]	Mars ambient atmospheric viscosity
R_1	0.2 m	Fan hub radius
R_2	1.2 m	Fan radius
B	3	Number of fan blades
c	0.3 m	Fan blade chord length
RPM	500 RPM	Rotation rate, revolutions per minute
ω	52.4 rad/s	Rotation rate
$V_{fan\ needed}$	18.2 m/s	Needed for 8 m/s flow rate at zeolite bed
$V_{fan\ actual}$	20.6 m/s	Determined as derived above
η_f	0.76	Fan efficiency

4.2 Pressure Drop Modeling

In order to calculate the power needed to drive the fan, it is necessary to determine the pressure drop of the flow across the filter and the zeolite bed:

$$\Delta P = \Delta P_{filter} + \Delta P_{bed}\,.$$

The pressure drop across the filter is proportional to the flow velocity and is dependent on the type of filter medium [28]. For the pressure drop calculations, a Filtrete Type G filter from 3M was chosen [28]. Filtrete is an electrostatically enhanced non-woven fiber and is available in numerous grades, each having a different filtration efficiency and associated pressure drop. For WAVAR applications on Mars, a Filtrete G-200 will provide at least 95% efficiency [17,28]. Based on Filtrete G-200 data, Coons, *et al*, determined a linear pressure drop correlation across this filter to be [17,28]:

$$\Delta P_{filter} = 127.46\,\rho\,V\,.$$

This relation gives pressure drop in Pascals provided fluid density ρ and fluid velocity V are in SI units. Filtrete has been reported to have a longer life and greater temperature stability than similar media and should be acceptable for the ambient conditions that the WAVAR will encounter on Mars [28].

The pressure drop across the zeolite bed is calculated using the Ergun pressure drop model [32]. The Ergun model expresses the pressure drop across the bed as:

$$\Delta p = \frac{fL\rho(\varepsilon V)^2}{D_p}$$

where f is the friction factor, L is the bed depth, ρ is the average freestream density, ε is the void fraction, V is average flow velocity, and D_p is the pellet diameter. The friction factor is defined as:

$$f = \left[\frac{1-\varepsilon}{\varepsilon^3}\right]\left[\frac{150(1-\varepsilon)}{\mathrm{Re}_p} + 1.75\right]$$

and the Reynolds number based on the average zeolite pellet diameter is:

$$\mathrm{Re}_p = \frac{\rho V D_p}{\mu}$$

where μ is the viscosity of the Martian atmosphere.

The current WAVAR design incorporates a zeolite bed 4 cm deep with a void fraction of 0.4, and a 3 mm average pellet diameter. An average atmospheric density of $\rho = 0.017$ kg/m^3 was assumed, based on an average temperature $T_{avg} = 210$ K and an average pressure $P_{avg} = 5$ torr. The viscosity was curve fit as a function of tem-

perature and found to be 1.08×10^{-5} N·s/m^2 at 210 K [33,34]. These parameters are sufficient to calculate both the filter and bed pressure drops as functions of flow velocity. The resulting total pressure drop as a function of Reynolds number at the zeolite bed, and the power required for fan operation are plotted in Fig. 16.

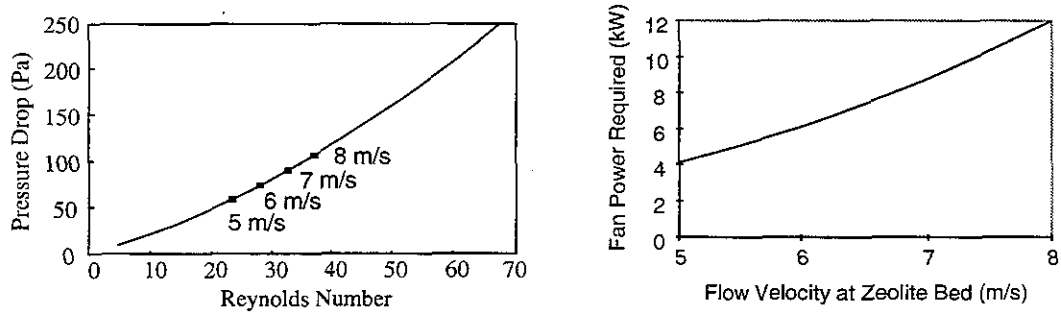

Fig. 16. Pressure drop as a function of Reynolds number at zeolite bed and power required for fan operation as a function of flow velocity at the bed. Pressure drop for the 4 cm deep bed was computed using a linear model for the filter pressure drop [17,28] and the Ergun model for the bed pressure drop [32]. Pressure drops at the zeolite bed corresponding to 5, 6, 7, and 8 m/s flow velocities are indicated.

The goal of the WAVAR is to produce an average of 3.3 kg of water per day, enough to replace the losses due to inefficiency in the life support system of the NASA Reference Mission. To meet this goal, the volume flow rate through the WAVAR must be sufficient to provide this average of 3.3 kg of water per day. Hence, the average atmospheric vapor concentration dictates the necessary volume flow rate through the WAVAR. However, the water vapor concentration depends strongly on temperature and varies with time of day, season, and latitude [9]. Thus it was necessary to find the average water vapor concentration at each of several locations on Mars and to calculate the average pressure drop at each of those locations, based on the average vapor concentration and corresponding volume flow rate. Once the pressure drop values were determined for certain flow rates, they were used to calculate the fan power required to pull the Martian atmosphere through the WAVAR's filter and zeolite bed. The results of these power calculations are discussed below.

4.3 Fan Power

Fan power requirements are determined from the fan efficiency and the pressure drop across the filter and zeolite bed. The fan efficiency and pressure drop are calculated as described above. Fan power is determined from:

$$Power = \frac{\Delta P \cdot Q}{\eta_m \eta_f}$$

where Q is the volumetric flow rate, η_m is the motor efficiency, and η_f is the fan efficiency. Values used in fan power calculations are summarized in Table 5. Results of fan power calculations are shown in Fig. 16.

Table 5. Constants used for performance calculations.

ρ_{amb}	Mars ambient density	1.7×10^{-2} kg/m^3
--	Zeolite bed void fraction	0.4
--	Zeolite pellet diameter	3 mm
η_m	Motor efficiency (assumed)	0.95
η_f	Fan efficiency	0.76

4.4 Simulation Performance

The primary quantities that characterize the effectiveness of the WAVAR are the total mass of water collected, the power and energy required for operation, and the mass of the WAVAR. In order to characterize the WAVAR's performance under a wide range of Martian atmospheric conditions, simulations were performed that take into account seasonal and diurnal fluctuations in the temperature and vapor concentration, the characteristics of zeolite, and the limitations set on system power by the design constraints.

The energy required by the WAVAR for extraction of a given mass of water depends upon the amount of time that the fan operates and the number of desorption cycles that occur. An initial comparison of WAVAR performance under different atmospheric conditions was carried out with a constant flow velocity through the zeolite bed of 7 m/s, requiring a constant fan power of 8.6 kW. Additional simulations were carried out under different atmospheric conditions with flow velocities of 5 m/s, 6 m/s and 8 m/s, each with a corresponding fan power. The energy required to desorb the water from the zeolite was assumed to remain the same for desorption cycles in all simulations since the loading fraction at which desorption begins is always the same.

Adsorption of water is dependent upon the instantaneous water vapor concentration, the instantaneous zeolite loading fraction, and the instantaneous zeolite capacity, as determined by the zeolite bed temperature. In the simulations it was assumed that all of the water vapor that passes through the zeolite bed is adsorbed.

To simulate variations in the atmospheric water vapor concentration, data from the Viking Landers and Viking Orbiters were used. Since the water vapor concentration data on the surface were inferred [9] and are uncertain, simulations were run using different concentration fluctuation models to obtain an envelope of performance. The only locations for which both temperature and concentration data are available are the two Viking Lander sites. The water vapor concentration inferred by Ryan, *et al* are in good correlation with the MAWD measurements at VL-1 but not at VL-2 [9]. It is possible that the correlation disparities at VL-2 are due to a non-uniform vertical distribution of water vapor [9]. Regardless, both of these sites were used in the simulations.

Since the average concentration measured by VL-1 was below the global average of $\sim 2.0 \times 10^{-6}$ kg/m^3 [6], two additional concentration profiles were assumed in order to obtain an envelope of performance for the WAVAR. First, the vapor concentration for VL-1 was scaled up so that the average concentration was equivalent to the global average. This data set is termed New Houston. Second, the vertical column abundance at the northern polar region is about 10 times that at lower latitudes during the summer [9]. However, during the winter the water column abundance is much lower at the north pole than at lower latitudes, so it was assumed that there is no appreciable water at any time other than summer. The simulation was run using a vapor concentration of eight times that measured by VL-1. The simulation was run for only 145 sols, in an attempt to simulate the high concentration during polar summer and extremely low concentration during other seasons.

The seasonal variations in water vapor concentrations from Viking 1 and 2, New Houston, and the northern polar region are shown in Fig. 17. Extremely low vapor concentrations were also measured during the winter by VL-2. An analysis of WAVAR performance over a full Martian year showed that during the period from Sol 146 through Sol 500 of VL-2, the WAVAR would collect less than 15 kg of water, while still requiring a constant 8.6 kW for operation (with 7 m/s flow rate through the zeolite bed). Therefore, the simulation for VL-2 conditions was only run through Sol 145.

There are no diurnal water vapor concentration fluctuation estimates, but the daily maximum and minimum concentrations are known. The daily maximum is the concentration that Ryan, *et al* [35] reported and the minimum is determined by using the 100% humidity restriction from the Clausius-Clapeyron equation [36] at the coldest part of the night. As described by Ryan, *et al* [9], when the temperature reaches the frost point, an inflection point occurs on a plot of temperature vs. time due to the energy released by water as it freezes. The atmosphere at the time of the inflection point may be assumed to be saturated. From the initial saturation time until when the temperature begins to rise the next morning, water vapor is being forced to precipitate out and is reported to be in the form of fog [9]. As the temperature begins to rise in the morning the fog and/or frost on the regolith returns to the atmosphere as vapor. The actual evaporation/sublimation rate is unknown but is estimated by the curve shown in Fig. 18. The saturation curve is shown along with the concentration from Ryan and the assumed daily variation in concentration.

The assumption that the atmospheric water content follows the 100% humidity level below the frost point

is probably pessimistic because as the temperature drops the water vapor precipitates out as fog. This fog would also be adsorbed by the WAVAR. However, since the amount and location of nighttime fog are unknown, simulations at each location are run under both the fog and no-fog assumptions. In the fog simulations, the concentration is more or less constant during the day and night, and is mainly influenced by seasonal effects. In the no-fog simulations, the atmospheric water content during the night follows the saturation curve below the frost point. Sample concentration curves for the fog and no-fog assumptions are shown in Fig. 18. Actual conditions on Mars probably lie somewhere between the fog and no-fog curves at each site.

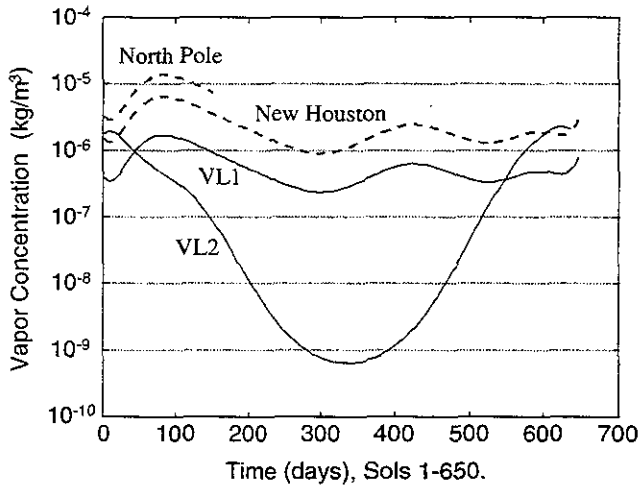

Fig. 17. Seasonal variation of vapor concentration as used in the simulations. Solid lines are actual data, dashed lines are estimated.

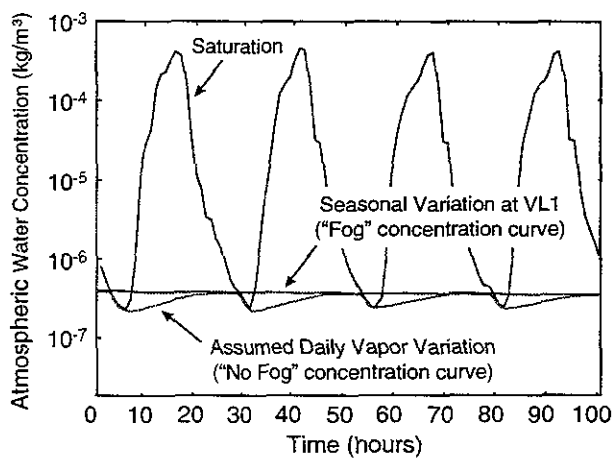

Fig. 18. Five sols of atmospheric water content data used in the VL-1 site simulation.

In the simulations, the desorption cycle was assumed to begin when the zeolite bed reached a loading fraction of 15%. Depending on temperature fluctuations, a loading fraction of over 18% could be achieved but the amount of time spent each day in thermal isolation during daytime capacity dips (daytime temperature peaks) increases at higher loading fractions, reducing the time available for adsorption and thus the mass of water adsorbed each day. A sample plot of the instantaneous amount of water adsorbed in the zeolite bed over one 300-hour period is shown in Fig. 19. The nearly vertical line occurs during a desorption cycle, when the loading fraction of the zeolite drops from 0.15 to 0.015 in only four hours. The wavy pattern is caused by diurnal fluctua-

tions in vapor concentration.

The specific energy required for water collection is calculated by dividing the total energy needed by the total mass of water extracted. The total energy is computed by multiplying the time spent adsorbing by the power draw of the fan and adding the number of desorption cycles times the energy needed to desorb the water from the zeolite bed.

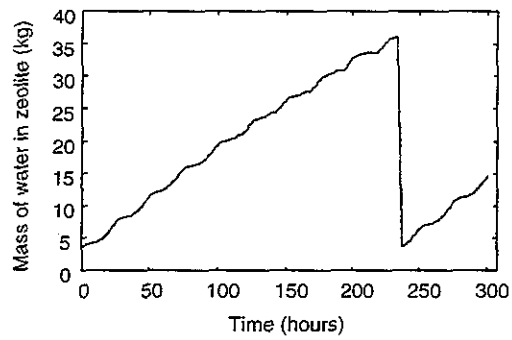

Fig. 19. Sample instantaneous water loading curve.

Tables 6 and 7 summarize the WAVAR simulation results for the four site models under the above-mentioned atmospheric conditions. The simulation at the VL-1 site is for only 333 sols, about ½ of a Martian year, because accurate temperature data are not available for a full year [37]. There is a period from Sol 117 through Sol 133 of VL-1 for which no temperature data are available, so the simulation skips these sols. New Houston concentration and temperature are based on VL-1 data, so the simulation at New Houston also runs for only 333 sols. Since the data used for the VL-1 and New Houston simulations correspond to the first half of the year, during which the vapor concentration is higher than the yearly average (see Fig. 17), the results may not be scaled linearly to obtain yearly results. The simulations for the VL-2 site and the North Pole are for the summer only because the water concentration is too low during the rest of the year for efficient WAVAR operation. The results from New Houston and the north pole represent total yearly returns, because the WAVAR would not be in operation during seasons with extremely low vapor concentration.

Overall performance at each site as a function of flow velocity at the zeolite bed is summarized in Figs. 20-22. Figure 20 shows the mass of water collected by the WAVAR per sol of operation. Figure 21 shows the average power required for WAVAR operation, and Fig. 22 plots the specific energy required. As is apparent from Tables 6 and 7 and Figs. 20-22, WAVAR performance is highly dependent on atmospheric water content.

Table 6. Simulation results under fog assumption with 7 m/s flow rate through zeolite bed.

Site	Number of sols simulated	Total mass of water collected (kg)	Average power during operation (kW)	Mass per sol of operation (kg/sol)	Mass per sol over year (kg/sol)	Specific energy (kW-hr/kg)
VL-1	333 *	1264	8.4	3.79	---	55.2
VL-2	145 †	616	8.7	4.25	0.96 †	52.6
New Houston	333 *	4730	9.8	14.21	---	17.3
North Pole	145 *†	5670	12.1	39.1	8.86 †	7.7

* Accurate temperature data is not available for Sols 117-133 or 351-640 of VL-1, so these sols were not included in the simulations based on VL-1 data.

† Simulations were run only during the summer, but correspond to a full year of operation since at these sites because the WAVAR only operates during seasons with high vapor concentration.

Table 7. Simulation results under no-fog assumption with 7 m/s flow rate through zeolite bed.

Site	Number of sols simulated	Total mass of water collected (kg)	Average power during operation (kW)	Mass per sol of operation (kg/sol)	Mass per sol over year (kg/sol)	Specific energy (kW-hr/kg)
VL-1	333 *	778	8.0	2.34	---	85.9
VL-2	145 †	421	8.5	2.90	0.66 †	74.9
New Houston	333 *	2041	8.9	6.13	---	36.2
North Pole	145 *†	1976	9.6	13.63	3.09 †	17.5

* Accurate temperature data is not available for Sols 117-133 or 351-640 of VL-1, so these sols were not included in the simulations based on VL-1 data.

† Simulations were run only during the summer, but correspond to a full year of operation since at these sites because the WAVAR only operates during seasons with high vapor concentration.

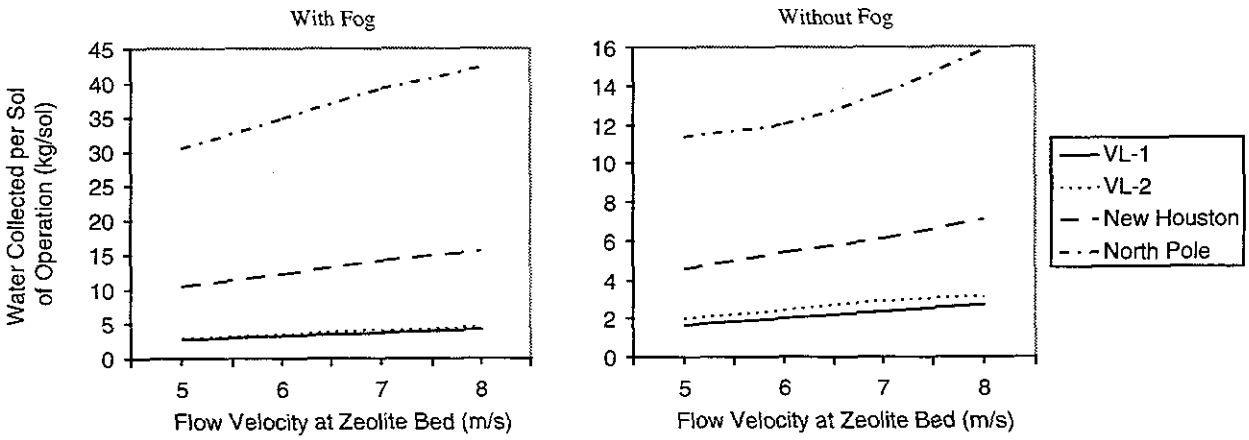

Fig. 20. Water collected by WAVAR per day of operation.

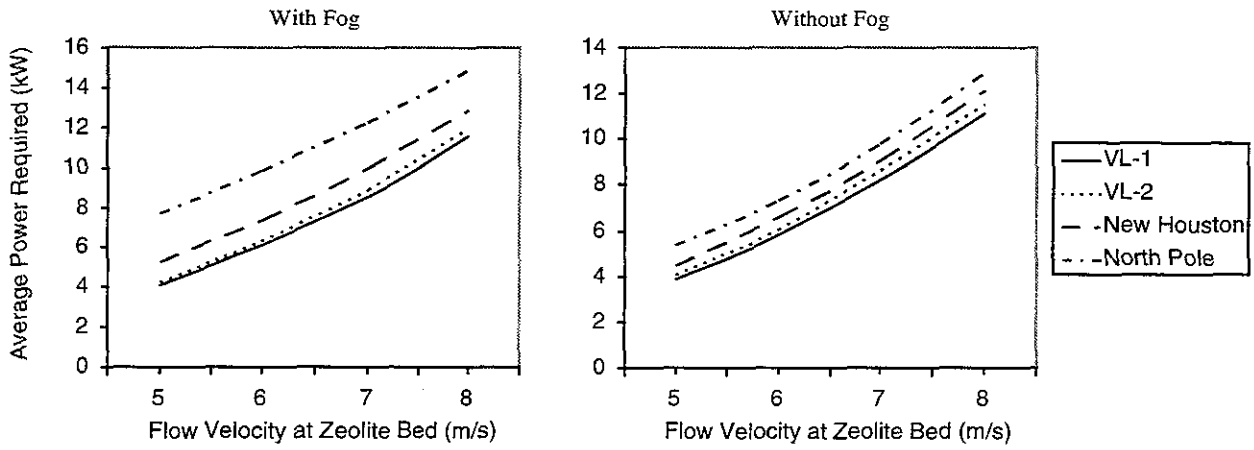

Fig. 21. Average power required for WAVAR operation.

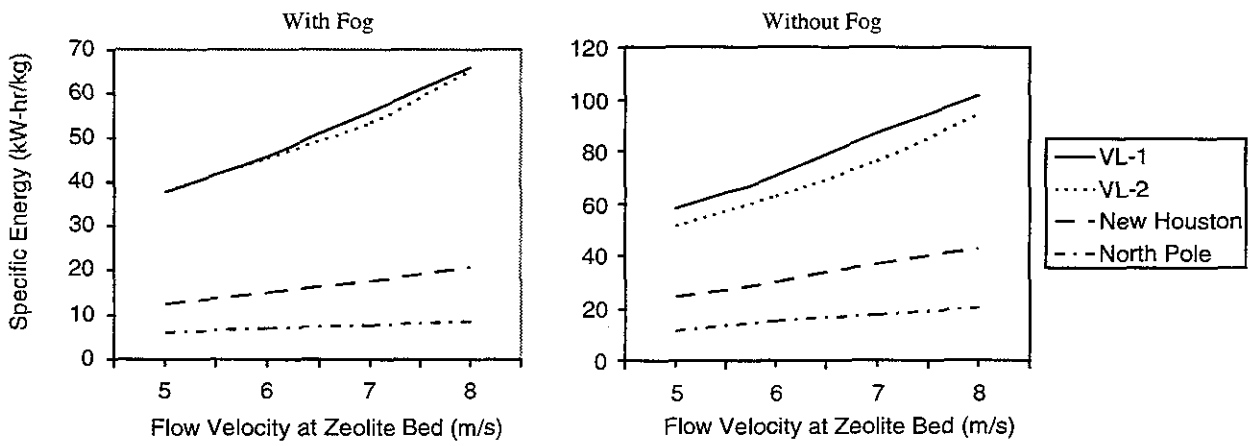

Fig. 22. Specific energy required for collection of water by the WAVAR.

5. CONCLUSION

Results from this study demonstrate that the WAVAR concept is a feasible method for replacing regenerative water losses from the life support system with indigenous water in NASA's Mars Reference Mission. The WAVAR design presented integrates into the Reference Mission in a configuration mounted on the top of the existing laboratory habitat module and has a total dry mass of 885 kg. Simulations show that the design has varying capability under different conditions on Mars. The four conditions simulated in the study are water vapor content and temperature fluctuations at the Viking Lander 1 site, the Viking Lander 2 site, the North Pole based upon Viking Orbiter data, and a hypothetical site called "New Houston" which is a site with daily fluctuation trends based upon those seen at the Viking Lander 1 site but with a average yearly water vapor concentration equivalent to the global average. Simulations were carried out at each site for conditions with and without nighttime. The results of the simulations show that for no-fog conditions the WAVAR meets the design requirements only at the New Houston and North Pole sites. Under the nighttime fog assumption, however, the WAVAR satisfies the requirements under VL-1, New Houston, and North Pole conditions. The low average power required for each of the successful cases suggests that an increase in fan power may be used to increase flow velocity and the rate of water adsorption without exceeding the power constraint of 5% of Reference Mission power. This would be espe-

cially beneficial at the North Pole, where an increase in average power to 15 kW increases the daily net gain of water to 42 kg/sol. Low vapor concentrations at the VL-2 site preclude efficient use of the WAVAR regardless of fog assumptions. The most efficient and productive site for WAVAR use is the northern polar region, where the vapor concentration is almost an order of magnitude higher than that measured at the VL-1 site during the summer. Under the New Houston with fog and North Pole with or without fog conditions, WAVAR performance is good enough to consider the complete replacement of seed hydrogen by the WAVAR in the NASA Reference Mission.

The results presented here were obtained using data of varying degrees of reliability. In order to perform a more rigorous simulation, the properties of zeolite 3A under the low pressures and temperatures on the Martian surface need to be determined experimentally. Tests are also needed to determine to what extent, if any, CO_2 blocks the adsorption of water in zeolite under runtime conditions. In addition, direct measurements of diurnal changes in the atmospheric water content at various sites on Mars are needed in order to determine the extent by which fog increases the water available for adsorption during periods of low ambient temperature.

ACKNOWLEDGEMENTS

The authors would like to extend their thanks to Seung Chung, Ben Diedrich, John Liptac, Doug MacSparran, Arti Nadkarni, Ryan Schwab, Andrew Shell, and Susana Quintana, all of whom participated in various aspects of the project. The authors are also indebted to Dr. Eckart W. Schmidt of Hazmat, Inc. for his encouragement and many helpful suggestions.

REFERENCES

1. Hoffmann, S.J, *et al*, *"Mars Reference Mission,"* NASA Johnson Space Center, Summer 1997.

2. Baker, D.A and Zubrin, R.M., "Mars Direct: Combining Near-Term Technologies to Achieve a Two-Launch Manned Mars Mission," *Journal of British Interplanetary Society*, 1990.

3. Ash, R.L., Dowler, W.L. and Varsi, G., "Feasibility of Rocket Propellant Production on Mars," Acta Astronomica, Vol. 5, 1978, pp. 705-724.

4. Connolly, J.C., Personal communication, Johnson Space Center, Jan 22, 1998.

5. Williams, J.D., Coons, S.C. and Bruckner, A.P., "Design of a Water Vapor Adsorption Reactor for Martian In Situ Resource Utilization," *Journal of British Interplanetary Society*, Vol. 48, pp. 347-354, 1995.

6. Carr, M.H., *Water on Mars*, Oxford University Press, Oxford, UK, 1996, pp. 3-46.

7. Jakosky, B.M., and Haberle, R.M., "The Seasonal Behavior of Water on Mars," in *Mars*, Kieffer, H.H., et al., eds., The University of Arizona Press, Tucson, 1992, pp. 969-1016.

8. Jakosky, B.M, and Farmer, C.B., "The Seasonal and global Behavior of Water Vapor in the Mars Atmosphere: Complete Global Results of the Viking Atmospheric Water Detector Experiment," *J. Geophys. Res.*, Vol. 87, 1982, pp. 2999-3019.

9. Ryan, J.A., Sharman, R.D., and Lucich, R.D., "Mars Water Vapor, Near Surface," *J. Geophys. Res.*, Vol. 87, 1982, pp. 7279-7284.

10. Smith, P.H., et al., "Results from the Mars Pathfinder Camera," *Science, Vol. 278*, 1997, pp.1758-1765.

11. Davies, D.W., "The Vertical Distribution of Mars Water Vapor," *J. Geophys. Res., Vol. 84*, 1979, pp. 2875-2879.

12. McKay, C.P., "Living and Working on Mars," The NASA Mars Conference, Reiber, D.B., ed., AAS Publications, San Diego, CA, 1988, pp. 516.

13. Ruthven, D.M., Shamshuzzaman, F., and Knaebel, K.S., *Pressure Swing Adsorption*, VCM Publishers, Inc., New York, NY, 1994, pp. 1-65.

14. Roussy, G., Zoulalian, A., Charreyre, M., and Thiebaut, J.M., "How Microwaves Dehydrate Zeolites," J. Phys. Chem., Vol. 88, 1984, pp. 5702-5708

15. Whittington, B.I., and Milestone, N.B., "The Microwave Heating of Zeolites," Zeolites, Vol. 12, 1992, pp. 815-818.

16. Coons, S.C., Williams, J.D., and Bruckner, A.P., "In Situ Propellant Production Strategies and Applications for a Low-Cost Mars Sample Return Mission," AIAA 95-2796, 31st AIAA/ASME/SAE/ASEE *Joint Propulsion Conference and Exhibit*, San Diego, CA July 10-12, 1995.

17. Coons, S.C., Williams, J.D., and Bruckner, A.P., "Feasibility Study of Water Vapor Adsorption on Mars for In Situ Resource Utilization," Paper AIAA 97-2765, 33rd AIAA/ASME/SAE/ASEE Joint Propulsion Conference, Seattle, WA, July 6-9, 1997.

18. Grover, M.R., Odell, E.H., Smith-Brito, S.L., Warwick, R.W., and Bruckner, A.P., "Project Ares Explore," Case for Mars VI, Boulder, CO, 1996, *In Press*.

19. Ferall, J.F., *et al*, "Life Support Systems Analysis and technical Trades for a Lunar Outpost", NASA-TM-109927, NASA Jet Propulsion Laboratory, Pasadena, CA, 1994.

20. Breck, D.W., *Zeolite Molecular Sieves*, Wiley-Interscience, New York, 1974.

21. Dyer, A., "An Introduction to Zeolite Molecular Sieves," John Wiley & Sons Ltd., Chistester, Great Britain, 1988, pp. 1-3.

22. "GRACE Davison Molecular Sieves Brochure for Zeolite 3A," W.R. Grace & Co., Baltimore, MD, (no date).

23. Roque-Malherbe, R., Personal communication, Instituto de Tecnologia Quimica UPV-CSIC, Universidad Politecnica de Valencia, Valencia, Spain, May 8, 1998.

24. UOP Technical Brochure UOP Molecular Sieves, UOP Molecular Sieve Adsobents, Garden Grove, CA, p. 10.

25. Marsh, K.N., "Recommended Reference Materials for the Realization of Physicochemical Properties," Blackwell Scientific Publications, Oxford, 1987, pg 256, Table 9.2.14.2.

26. Ishimaru, *Electromagnetic Wave Propagation, Radiation and Scattering*, John Wiley & Sons, New York, 1991, pp. 90-110.

27. Niu, M.C-Y., *Composite Airframe Structures*, Conmilit Press Ltd, Hong Kong, 1992, pg. 131.

28. Purchas, D., Handbook of Filter Media, Elsevier Advanced Technology, Oxford, UK, 1996, pp. 214-216.

29. NASA Commercial Technology Network, http://technology.ksc.nasa.gov/WWWaccess/Opport/aerogel.html

30. McCormick, B.W., *Aerodynamics, Aeronautics, and Flight Mechanics*, John Wiley & Sons, New York, 1995, pp. 298-300.

31. Laitone, E.V., "Aerodynamic Lift at Reynolds Numbers Below 7×10^4," AIAA Journal, Vol. 34, No. 9, Sept. 1996, pp. 1941-1942.

32. Ruthven, D. M., *Principles of Adsorption and Adsorption Processes*, John Wiley & Sons, New York, 1984, pp. 206-207.

33. Hirschfelder, J. O., Curtiss, C. F., and Bird, R. B., *Molecular Theory of Gases and Liquids*, John Wiley & Sons, New York, 1954, pp. 1122, 1126.

34. Svehla, R. A., "Estimated Viscosities and Thermal Conductivities of Gases at High Temperatures," Technical Report R-132, Washington National Aeronautics and Space Administration, 1963, pp. 21, 68, B2.

35. Ryan, J.A., and Sharman, R.D., "H_2O Frost Point Detection on Mars?," *J. Geophys. Res.*, Vol. 86, 1981, pp. 503-511.

36. Moelwyn-Hughes, E.A., Physical Chemistry, 2nd ed., Pergamon Press, Oxford, UK, 1961, pp. 275-279.

37. Kieffer, H.H., Jakosky, B.M., Snyder, C.W. and Matthews, M.S. editors, *Mars*, University of Arizona Press, Tucson, AZ, 1992, pg. 842.